JOURNAL OF INTERFERON & CYTOKINE RESEARCH
Volume 34, Number 1, 2014

DOI: 10.1089/jir.2012.0160

Crystal Structure of the Interferon Gamma Receptor Alpha Chain from Chicken Reveals an Undetected Extra Helix Compared with the Human Counterparts

Zhiguang Ping,[1,2] Jianxun Qi,[3] Yanling Sun,[4] Guangwen Lu,[3] Yi Shi,[3] Xiaojia Wang,[1] George F. Gao,[3,5] and Ming Wang[1,6]

Interferon gamma (IFN-γ) is an important cytokine that induces antiviral, antiproliferative, and immunomodulatory effects on target cells, and is also crucial in the early defense against intracellular parasites, such as *Listeria monocytogenes* and *Toxoplasma gondii*. The biological activity of IFN-γ relies upon the formation of a complex with its 2 receptors, the interferon gamma alpha chain (IFNGR1) and beta chain (IFNGR2), which are type II cytokine receptors. Structural models of ligand–receptor interaction and complex structure of chicken IFNs with their receptors have remained elusive. Here we report the first structure of *Gallus gallus* (chicken) IFNGR1 (chIFNGR1) at 2.0 Å by molecule replacement according to the structure of selenomethionine substituted chIFNGR1. The structural comparison reveals its structural similarities with other class II cytokine receptors, despite divergent primary sequences. We further investigate the ligand–receptor interaction properties of chicken IFN-γ (chIFN-γ) and chIFNGR1 using size-exclusion chromatography and surface plasmon resonance techniques. These data aid in the understanding of the interaction of chicken (avian) IFN-γ with its receptors and its signal transduction.

Introduction

Type II interferon (IFN), namely, interferon gamma (IFN-γ), is an important cytokine that induces antiviral, antiproliferative, and immunomodulatory effects on target cells (Farrar and Schreiber 1993) and is produced by activated Th1 CD4+ cells (Mosmann and Coffman 1989), CD8+ cells (Sad and others 1995), and natural killer cells (Perussia 1991). IFN-γ can be distinguished from type I (IFN-α, IFN-β, IFN-ε, IFN-κ, IFN-ω, and IFN-τ), and type III (IFN-λ) IFNs by its structure, receptor binding and immunological functions. The biological effects of the three IFN subfamilies rely on their binding to counterpart receptors: IFNAR1 and IFNAR2 for type I IFNs, IFNGR1 and IFNGR2 for type II IFN, and IFN-λR1 and IL-10R2 for type III IFNs (Gao and others 2009). IFN-γ is crucial in the early defense against intracellular parasites, such as *Listeria monocytogenes* and *Toxoplasma gondii* (Buchmeier and Schreiber 1985; Suzuki and others 1988; Portnoy 1992), and its receptors belong to the class II cytokine receptor (CRF2) family, which also includes other members: IL-10 receptors (IL-10R1 and IL-10R2), IL-22 receptors (IL-22R1 and IL-22BP), and IL-20 receptors (IL-20R1 and IL-20R2), and so on (Kotenko 2002; Langer and others 2004). Signaling through the cytokine pathway cascade is initiated when the cytokine binds to their corresponding receptor. It has been demonstrated that an IFN-γ dimer interacts with 2 molecules of IFNGR1 (Fountoulakis and others 1992; Chene and others 1995; Walter and others 1995) and is further stabilized by 2 molecules of IFNGR2 (Marsters and others 1995), which facilities complex stability by interacting with IFNGR1 but not with the ligand (Grayfer and Belosevic 2009).

The *Gallus gallus* (chicken) interferon gamma (chIFN-γ) gene was cloned from a cDNA expression library generated from a T cell line and identified through its antiviral activity and immunoregulated macrophage activities (Digby and

[1]National Animal Protozoa Laboratory, Key Laboratory of Animal Epidemiology and Zoonosis of the Ministry of Agriculture, College of Veterinary Medicine, China Agricultural University, Beijing, China.
[2]Laboratory of Noncoding RNA, Institute of Biophysics, Chinese Academy of Sciences, Beijing, China.
[3]CAS Key Laboratory of Pathogenic Microbiology and Immunology, Institute of Microbiology, Chinese Academy of Sciences, Beijing, China.
[4]State Key Laboratory of Biomembrane and Membrane Biotechnology, Institute of Zoology, Chinese Academy of Sciences, Beijing, China.
[5]Research Network of Immunity and Health (rNIH), Beijing Institutes of Life Science, Chinese Academy of Sciences, Beijing, China.
[6]Zhongmu Institutes of China Animal Husbandry Group, Beijing, China.

Lowenthal 1995; Song and others 1997). Chicken IFNGR1 (chIFNGR1) protein was generated and its physical characteristics were determined by mass spectrometry and circular dichroism (CD) spectrometry (Han and others 2006). Chicken IFNGR2 (chIFNGR2) was cloned using rapid amplification of cDNA 5′ and 3′ end (5′ and 3′ RACE) method and the secondary structure of its protein was identified by CD spectropolarimeter analysis (Han and others 2008).

Over the past decades, with the growth of biotechnology, such as CD spectroscopy, surface plasmon resonance (SPR), isothermal titration calorimetry, nuclear magnetic resonance (NMR), and X-ray diffraction, and others, it has become feasible to elucidate ligand–receptor interactions and structure properties of cytokines with their receptors. Human IFN-γ (huIFN-γ) binds IFNGR1 with high affinity (10^{-9}–10^{-10} M) (Aguet and others 1988; Bach and others 1995; Walter and others 1995), and the crystal structure of the complex has been shown to have 2 molecules of IFNGR1 bind to the homodimer of IFN-γ forming a 2:1 complex, where the receptor molecules do not interact with one another and are separated by 27 Å (Walter and others 1995). Moreover, the crystal structure complex of glycosylated extracellular part of IFNGR1 bound to IFN-γ, in addition to the expected 2:1 complex, revealed the presence of a third receptor molecule not directly associated with the IFN-γ dimer, thereby forming 3:1 complex with its ligand IFN-γ (Thiel and others 2000). Recently, the structure of human IFN-λ1 complexed with human IFN-λR1 was determined at a 1:1 molar ratio (Miknis and others 2010). Further, the complex structure of human IL-10 with human IL-10R1 showed that the complex consisted of 2 IL-10s and 4 IL-10R1 molecules (Josephson and others 2001), and a putative IL-22 with human IL-22R1 complex was proposed based on the crystal structure of IL-22/IL-22R1/IL-10R2 complex model (Bleicher and others 2008). Therefore, the current data regarding the complexes formed between cytokines and their receptors suggests that the architecture of their interactions may govern the process of initial recognition of the signaling transduction pathway cascade.

So far, although there have been many studies on huIFN-γ and its receptors, there has been no report illustrating chIFN-γ/chIFNGR1 interaction and the structural basis of the ligand–receptor complex of chIFN-γ with its receptor remains elusive. Chicken, like fish and frog have not only become vertebrate models for the study of infectious diseases and tumors, but also, they are present at key positions in evolution and contribute significantly to studies related to development and comparative analysis of immune system function and development (Savan and others 2009). Consequently, it is meaningful to elucidate the interaction and structural properties between chIFN-γ and its receptors.

In the present study, we report the 2.0 and 2.5 Å X-ray crystal structure of selenomethionine (Se-Met) substituted and native chIFNGR1, respectively. Comparison of the high-resolution structure chIFNGR1 with those of other type II cytokine receptors showed it is highly conserved between chicken and human, although there are considerable differences in their primary amino acid sequences. To elucidate the interaction relationship between chIFN-γ and chIFNGR1, analytical size-exclusion chromatography and SPR techniques were used. We propose that a plausible model for the interaction of chicken (avian) IFN-γ with its receptors.

Materials and Methods

Cloning, protein expression, and purification

The chIFN-γ gene (GenBank accession No. AY163160.1) was amplified as described previously (Song and others 1997), C-terminal (residues 19–164) was subcloned into fusion vector pGEX-6p-1 (GE Healthcare) with an N-terminal GST-tag, a unique *Bam*HI restriction site, a C-terminal stop codon, and a unique *Xho*I restriction site. The recombinant plasmids were transformed into *Escherichia coli (E. coli)* Rossetta-gami 2 (DE3) (Novagen), and expressed as soluble fusion proteins (GST chIFN-γ). Cells were harvested and lysed by an ultrasonic cell crusher with ice-cold phosphate buffer (pH 7.4), and then were centrifugated at 2,000*g* for 15 min at 4°C. The supernatant of lysate was applied into glutathione-Sepharose 4B (GE Healthcare) beads, after washing, soluble GST chIFN-γ was eluted by on-column cleavage with PreScission Protease (GE Healthcare) for 16 h at 4°C. The preliminary purified proteins were applied onto a Superdex 75 (GE Healthcare) size-exclusion column with ÄKTA purifier (GE Healthcare) for further purification.

ChIFNGR1 gene (GenBank accession No. NP_001123859.1) was constructed by our research group, previously (Han and others 2008; Ping and others 2012). The extracellular domain of chIFNGR1 (residues 28–234) was cloned into pET-21a vector (Novagen) with the restriction sites *Nde*I and *Xho*I, and a stop codon was used in C-terminal. Recombinant plasmids were transformed into *E. coli* strain Rossetta (DE3) and B834 (DE3) (Novagen) for the expression of native chIFNGR1 and Se-Met substituted chIFNGR1 (Se-Met chIFNGR1), respectively. Both of them were then expressed in inclusion bodies. The Se-Met chIFNGR1 was expressed using a modified methionine pathway inhibition procedure (Begley and others 2003). Transformed *E. coli* Rossetta (DE3) cells were grown at 37°C in 2×YT media (50 μg/mL ampicillin) to an optical density at 600 nm (OD_{600}) about 0.6–0.8. Cells were harvested by centrifugation at 1,500*g* for 15 min and washed twice with M_9 media [one liter of 10×M_9 salts contains 60 g of disodium hydrogen phosphate, 30 g of monopotassium phosphate, 5 g of sodium chloride (NaCl), and 10 g of ammonium chloride; pH 7.4], and then resuspended in M_9 media (50 μg/mL ampicillin) supplemented with 100 mg/L (Lys), 100 mg/L (Thr), 100 mg/L (Phe), 50 mg/L (Leu), 50 mg/L (Ile), and 50 mg/L (Val). Cell cultures were then grown for 15 min at 37°C to exhaust any residual methionine and 100 mg/L Se-Met was added. Isopropyl β-D-thiolgalactoside was added to a final concentration of 1 mM and protein was expressed at 37°C for 6 h. Complete substitution of methionine for Se-Met was confirmed by amino acid analysis. Se-Met-substituted chIFNGR1 was purified as described for native chIFNGR1.

For chIFNGR1 refolding, the procedure was done as described previously (Ping and others 2012). Briefly, cell pellets containing the inclusion bodies were harvested and washed three times with a buffer containing 0.5% v/v Triton X-100 [50 mM Tris-HCl (pH 8.0), 300 mM NaCl, 10 mM ethylene diamine tetraacetic acid (EDTA), and 10 mM DL-dithiothreitol (DTT)], and then once with the same buffer without Triton X-100. The inclusion bodies were dissolved overnight in 6 M Gua-HCl [with 50 mM Tris-HCl (pH 8.0), 100 mM NaCl, 10 mM EDTA, 10% glycerol, and 10 mM DTT] using 1 mL of buffer per 30 mg inclusion bodies. The chIFNGR1 was refolded by the gradual dilution method using refolding

buffer [100 mM Tris-HCl (pH 8.0), 400 mM L-arginine-HCl, 2 mM EDTA, 5 mM reduced glutathione, 0.5 mM oxidized glutathione, and 0.5 mM sodium azide] for 24 h at 4°C. After refolding, the chIFNGR1 proteins were concentrated and purified using a Resource Q (GE Healthcare) column and Superdex 75 (GE Healthcare) column for ion-exchange and size-exclusion chromatographies, respectively.

Crystallization, data collection, and processing of Se-Met chIFNGR1

The purified Se-Met chIFNGR1 was crystallized according to the native chIFNGR1 procedure (Ping and others 2012). The crystals of Se-Met chIFNGR1 were obtained in 20% (v/v) polyethylene glycol 5000 monomethyl ether, 0.1 M 4-(2-hydroxyethyl)-1-piperazineethanesulfonic acid (HEPES), and 0.5 M sodium carbonate (pH 7.0). For data collection, the crystals were cryoprotected in mother liquor containing 20% glycerol before being flash cooled directly in liquid nitrogen. Diffraction data were collected on beam line BL17U1 (100 K, wavelength 0.98 Å) of Shanghai Synchrotron Radiation Facility. The data were processed and scaled using the HKL2000 software package (Lake and others 1997).

Structure solution, refinement, and analysis

The crystal structure of Se-Met-IFNGR1 was firstly solved by the method of multiwavelength anomalous diffraction (Hendrickson and others 1990) by phase determining with Se-Met molecules. The structure of native chIFNGR1 was determined by molecular replacement method using Phaser (Read 2001) from the CCP4 program suite (Collaborative Computing Project 1994) using the structure of Se-Met chIFNGR1 as the model. The different residues between native chIFNGR1 and Se-Met chIFNGR1 were manually rebuilt in the program COOT under the guidance of F_o–F_c and $2F_o$–F_c electron density maps (Emsley and Cowtan 2004). Consequently, the initial rigid body and a series of restrained translation/libration/screw (TLS) refinements were performed with the REFMAC5 program (Murshudov and others 1997). All of the structures were further refined by additional rounds of refinements using the PHENIX package (Adams and others 2002), with coordinate refinement, isotropic atomic displacement parameters (ADP) refinement, and bulk solvent modeling. The stereochemical quality of the final model was assessed with the PROCHECK program (Laskowski and others 1993). All structural figures were generated using PyMOL (DeLano 2002).

Mutagenesis of putative ligand binding sites of chIFNGR1

The chIFNGR1 mutations were subcloned using polymerase chain reaction (PCR) using recombinant plasmid chIFNGR1/pET-21a as previously report (Wei and others 2004), 2-step overlapping PCR was performed for 2 cycles using QuikChange® Site-Directed Mutagenesis Kit (Stratagene), and then *Dpn*I (New England Biolabs) was added to the mixture to overdigest the methylated template for 90 min at 37°C. After that, 2.5 μL digestion product was transformed to Rossetta (DE3). All the mutations were expressed and purified according to the method of wild-type chIFNGR1, and the buffer of size-exclusion chromatographies was phosphate buffer (pH 7.4).

Table 1. X-Ray Crystallographic Data Collection and Refinement Summary Statistics

	Native-chIFNGR1	*Se-Met chIFNGR1*
Data collection		
Space group	$P6_522$	$P6_522$
Wavelength	0.97931	0.97908
Unit cell dimensions		
a, b, c (Å)	63.5, 63.5, 216.3	63.6, 63.6, 215.8
α, β, γ (°)	90, 90, 120	90, 90, 120
Resolution (Å)	50.00–2.50 (2.59–2.50)	50.00–2.00 (2.07–2.00)
Observed reflections	228,123	361,378
Completeness (%)	99.3 (93.7)	96.8 (100.0)
Redundancy	23.6 (16.0)	35.8 (32.6)
R_{merge} or R_{sym}	0.105 (0.396)	0.143 (0.469)
I/σ (*I*)	5.4 (4.7)	20.6 (14.3)
Refinement		
Resolution (Å)	38.57–2.50	38.54–2.00
Number of reflections	9,050	17,153
Completeness for range (%)	93.80	93.34
R_{work}/R_{free}	0.2180/0.2664	0.2334/0.2602
No. atoms		
Protein	1,643	1,643
Water	23	221
B-factors (Å^2)		
Protein	53.9	34.7
Water	55.9	37.6
Root-mean-square deviations		
Bond length (Å)	0.004	0.014
Bond angles (°)	0.811	1.288
Ramachandran plot (%)		
Most favored regions	90.1	89.0
Additional allowed regions	8.2	9.90
Generously allowed regions	1.1	0.5
Disallowed regions (%)	0	0
PDB ID	4EQ2	4EQ3

Values in parentheses are for the highest-resolution shell.
PDB ID, protein data bank identification.

SPR analysis between chIFN-γ and chIFNGR1

SPR was performed using Biacore® 3000 (GE Healthcare) to determine the interaction of chIFN-γ and chIFNGR1 (Cooper 2003; Sitlani and others 2007). Purified chIFNGR1 was coupled to a research-grade carboxymethylated dextran sensor chip (CM5; GE Healthcare) to give surface densities of ~1,500 resonance units (RU). ChIFN-γ proteins were injected with the concentration of 0, 15.625, 31.25, 62.5, 125, and 250 nM in a solution of 10 mM HEPES (pH 7.4), 150 mM NaCl, and 0.005% surfactant P20. The surfaces of sensor chip were regenerated with 15 mM sodium hydroxide and all of the injections were performed at 25°C with the flow rates of 5 μL/min. The data of measurements were recorded with real-time and analyzed by BIAevaluation software version 4.1, and then fit by assuming a simple 1:1 Langmuir binding model.

For the determination the interaction of chIFNGR1 mutations with chIFN-γ, the chIFN-γ (residues 19–164) was subcloned into pET-28a vector (Novagen) with the

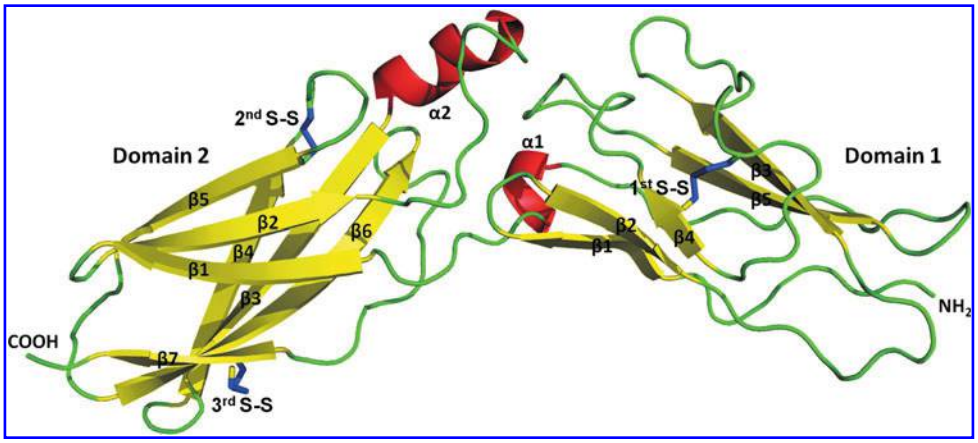

FIG. 1. The ribbon diagram of chIFNGR1 structure. An overall view the crystal structure of chIFNGR1 displays as 2 domains: D1 and D2, which contain 5 and 7 yellow-colored β-sheets, respectively. Helices are colored in red. Three disulfide bridges link counterpart molecules are indicated as blue sticks. chIFNGR1, *Gallus gallus* (chicken) IFNGR1; IFN, interferon.

N-terminal His-tag, which was purified by Ni-NTA column (Novagen) and washed by gradient imidazole, the Superdex 75 (GE Healthcare) size-exclusion column with phosphate buffer (pH 7.4) was used for further purification. SPR analyses were still performed by using Biacore 3000 equipped with Sensor Chip CM5. First, His_4 mAb surfaces were prepared by using standard procedures (Rich and others 2002), ~13,000 RU antibody immobilized on the chip. Second, the ligand chIFN-γ/His (20 μg/mL) was injected across immobilized His antibody, resulting in the capture of ~1,700 RU ligand. Third, 1 μM of each mutation of chIFNGR1 and the wild type were injected over antibody-captured chIFN-γ/His. The ligand/receptor complexes were stripped for regeneration with elution buffer: 10 mM phosphoric acid. The binding status was recorded and analyzed by BIAevaluation software version 4.1.

Results

Overall structure of chIFNGR1

Due to the limited sequence identities of chIFNGR1 with IFN receptors of known structures, our initial molecular replacement trials failed. The presence of 3 methionine in the protein sequence reminds us that the Se-Met-based single wavelength anomalous diffraction (SAD) method could be used to solve the phase problem. Finally, all the 3 methionine sites were successfully located, based on which a model of

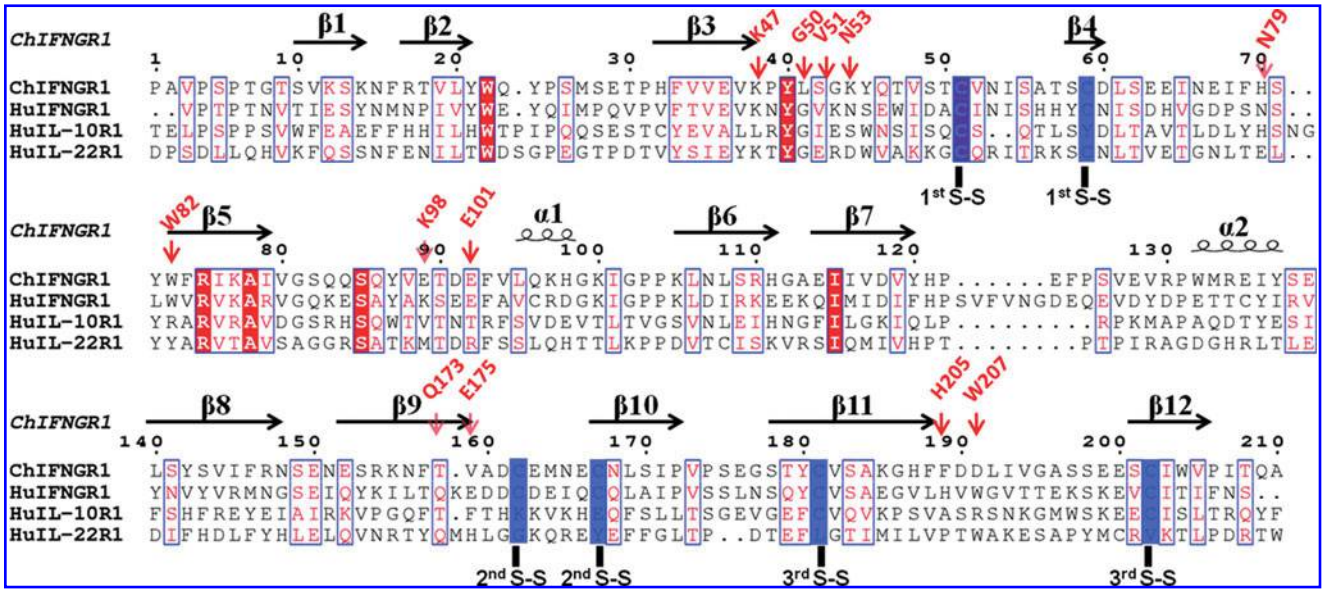

FIG. 2. Multiple sequence alignment of select members of the type II cytokine receptors family, including chIFNGR1, huIFNGR1, huIL-10R1, and huIL-22R1. The numbering used for huIFNGR1, huIL-10R1, and huIL-22R1 is aligned on the numbering of the sequence of chIFNGR1. The secondary structures are indicated for each sortase with black *arrows* (β-sheets) and black coil (α-helices). The similar sequence of chIFNGR1 and huIFNGR1 was shown with red square. The red shading indicates the region that is conserved in all compared sequences, and the blue square indicates the identity >50% in all sequences. Three disulfides bonds in the chIFNGR1 molecule were labeled in the following of their correspondence sequence. The residues marked in red indicate the binding sites of huIFNGR1 with its ligand huIFN-γ. The sequences were aligned using ClustalW2 (http://ebi.ac.uk/Tools/msa/clustalw2/) and similarity scores were presented by ESPript 2.2 (http://espript.ibcp.fr/ESPript/ESPript/). huIFNGR1, human IFNGR1.

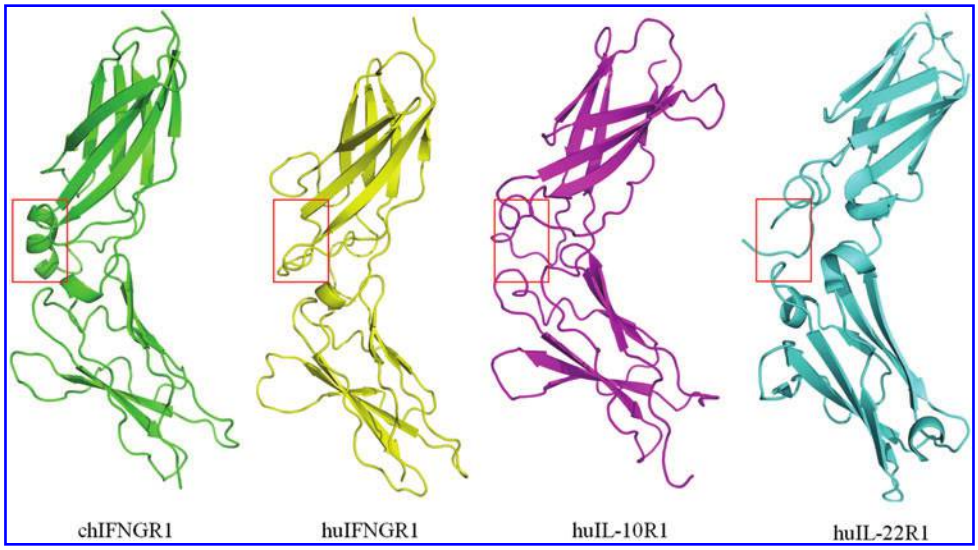

FIG. 3. The structures of type II cytokine related receptors. Structural comparison of the 4 type II cytokine related receptors, chIFNGR1, huIFNGR1, huIL-10R1, and huIL-22R1. The structures of chIFNGR1 (green), huIFNGR1 (yellow), huIL-10R1 (magenta), and huIL-22R1 (cyan) are superimposed. The ribbon structures were displayed with PyMOL (DeLano Scientific; http://pymol.org). Protein Data Bank (PDB) code of huIFNGR1: 1FG9; huIL-10R1: 1J7V; huIL-22R1: 3DLQ.

good stereochemistry was built. The final structure was refined to $R_{work} = 0.2334$ and $R_{free} = 0.2602$, respectively (Table 1). Single crystals of native and Se-Met chIFNGR1 were successfully obtained, which could diffract to 2.5 and 2.0 Å resolution, respectively (Ping and others 2012). The solved structure, with 207 residues being visible in the electron density map, contains 2 Ig-like domains (D1 and D2) connected by a flexible linker (residues 126–131) (Fig. 1). The D1 domain is composed of N-terminal residues 28–125 and forms a β sandwich structure with a layer of 5 β-strands. In contrast to domain D1, the D2 domain of chIFNGR1, which includes 103 amino acids from 132 to 234, forms a 7-stranded β sandwich structure. There are 3 disulfides: C51&C59 in D1 domain, C162&C167, and C181&C202 in D2 domain (Fig. 1). Three methionine residues, one located in the D1 domain remaining two located in the D2 domain, were substituted with Se-Met to help determine the phase of the chIFNGR1 structure. The structure of chIFNGR1 reveals that this protein is largely formed by β-strands, with only 13 residues forming 2 α-helices (Fig. 1).

Comparison of the 3-dimensional structure of chIFNGR1 with other cytokine receptors

Alignment of primary sequences reveals that chIFNGR1 has lower identity with other class II cytokine receptors, including huIFNGR1, huIL-10R1, and huIL-22R1 (Fig. 2). Nevertheless, the 3-dimensional structures of these proteins are quite similar with each other. Structural comparison of chIFNGR1 with huIFNGR1 reveals that chIFNGR1 almost shares the similar structure with its human counterpart (Fig. 3), although their sequence identity shows just about 30% (Fig. 2). The structure comparison onto those of huIFNGR1, huIL-10R1 and huIL-22R1, showed they almost share the same structure with chIFNGR1 (Fig. 3). With the root-mean-square deviation (RMSD) was varied according to the comparison of chIFNGR1 with other cytokine receptors (Table 2). However, a remarkable additional α-helix located in D2 domain was detected in chIFNGR1, which was absent in other counterparts, and the $2F_o–F_c$ electron density map of which was shown in Fig. 4.

Table 2. The Root-Mean-Square Deviation Comparison of chIFNGR1 with Other Cytokine Receptors

	Domain I (RMSD)	*Domain II (RMSD)*
chIFNGR1 vs. huIFNGR1	1.409 (60 Cα)	0.876 (87 Cα)
chIFNGR1 vs. huIL10-R1	2.152 (62 Cα)	1.257 (70 Cα)
chIFNGR1 vs. huIL22-R1	4.472 (42 Cα)	0.936 (67 Cα)

RMSD, root-mean-square deviation.

Structural alignment of this newly obtained chIFNGR1 structure with the huIFNGR1 reveals the well-aligned Ig-like domain, but relative differences lies in the interdomain angles between them. As shown in Fig. 5, with the longitudinal axis crossing the first Ig domain of huIFNGR1 as reference, the orientation of the chIFNGR1 structure could be rotated about 30.9°. This observation indicates that the relatively flexible interdomain linker for the 2 domains in the IFNGR1 structure, which is similar with the PD-L1 structure (Chen and others 2010).

The complex structure of human IFN binding to its receptor IFNGR1 has been reported by Thiel and others (2000) previously. In this structure, 12 residues in huIFNGR1 are identified as the key players involved in the ligand–receptor interaction. Most of these residues are located in the loop regions, which include "the β3-β4 loop" and "the β4-β5 loop" in D1 domain, and "the β2-β3 loop," "the β4-β5 loop," and "the β6-β7 loop" in D2 domain. For this ligand-binding related loop, chIFNGR1 exhibit a quite similar loop as that of the huIFNGR1. Twelve ligand binding sites were found by analyzing the complex structure of huIFNGR1 with huIFN-γ (Fig. 6), which were gathered together in the loop region. chIFNGR1 has similar loop region to huIFNGR1, which contains the majority of binding sties K38A, L41A, S42A, K44A, H70A, W73A, E89A, E92A, and F189A, which help chIFNGR1 anchoring to its ligand huIFN-γ. However, 3 other binding sites T158A, V159A, and D191A, show a large conformational change in chIFNGR1 and huIFNGR1 structures (Fig. 6). The conformational change may occur to allow for the interaction of amino acids between chIFNGR1 and chIFN-γ in the binding site, although the similar region between chIFNGR1 and huIFNGR1 in the binding site does not show this configuration.

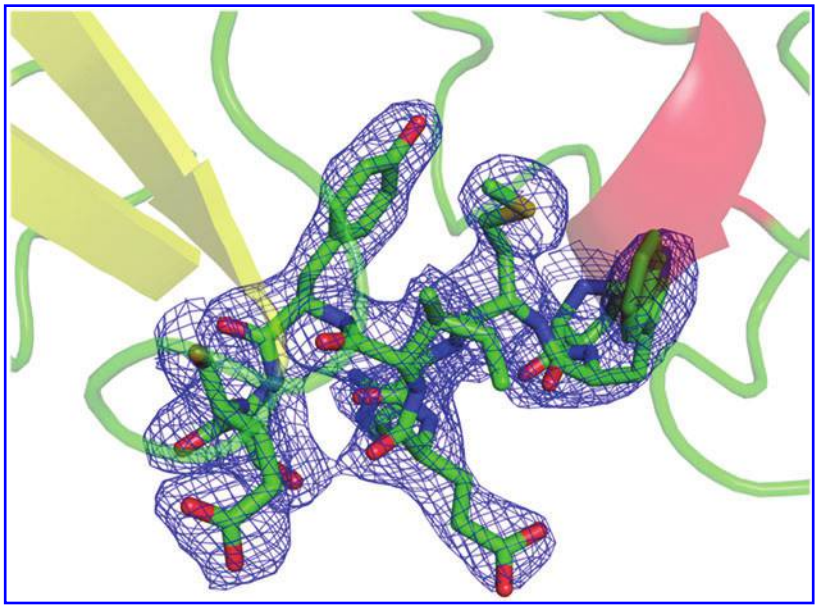

FIG. 4. The $2F_o$–F_c electron density map of the α2-helix of chIFNGR1 structure which is absent in the other type II cytokine receptors.

Interaction characterization of soluble chIFN-γ with chIFNGR1

Without a complex structure of chIFN-γ binding to chIFNGR1, we cannot define the detailed residue-by-residue interaction mediating intimate interaction between the 2 molecules. Nevertheless, the sequence alignment result shows that 9 (out of 12) amino acids involved in ligand binding in huIFNGR1 are also conserved in the chicken receptor.

A 1:1 binding mode of chIFN-γ with chIFNGR1 was obtained using analytical size-exclusion chromatography with Superdex®75 10/300 GL column (GE Healthcare). As shown in Fig. 7, purified chIFN-γ and chIFNGR1 were eluted as a single peak at 12.96 and 10.99 mL, corresponding to an apparent molecular weight (M_W) of about 17 and 24 kDa, respectively. This result demonstrates that both chIFN-γ and chIFNGR1 exist as a homogeneous monomer in solution. *In vitro* mixture of chIFN-γ with chIFNGR1 yield a stable complex, which behaves as a single peak with an elution volume of about 10.08 mL. The molecular weight of the complex was calculated to be about 40 kDa, which is in good accordance with the M_W of one chIFN-γ molecule in combination with a single chIFNGR1. We further demonstrated the identity of the complex by 15% sodium dodecyl sulfate polyacrylamide gel electrophoresis (SDS-PAGE) (Fig. 7).

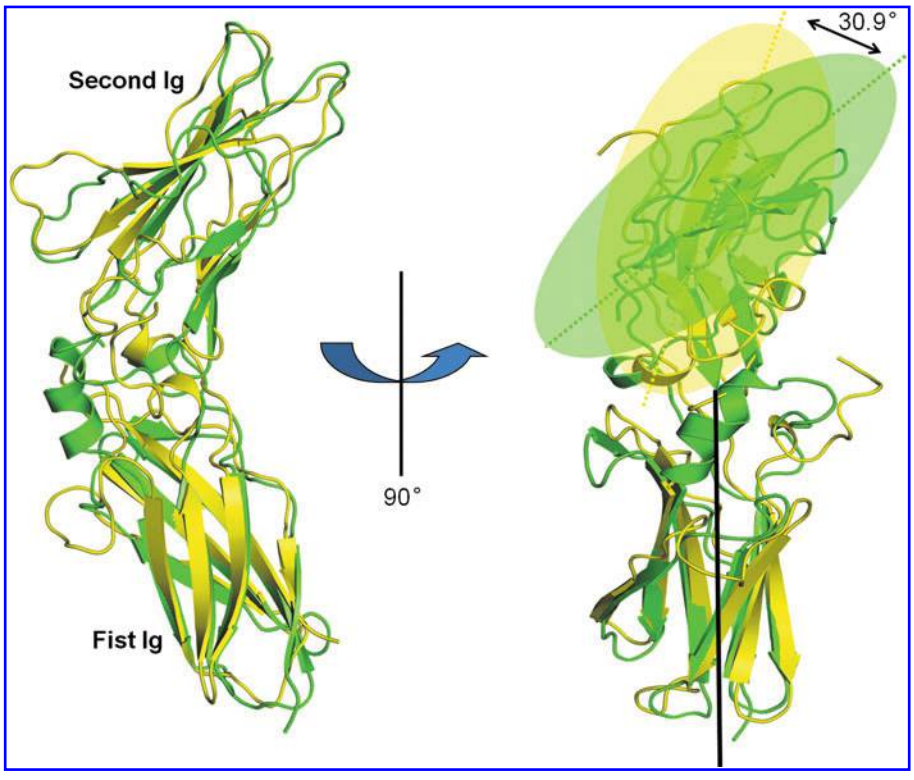

FIG. 5. The superimposition of chIFNGR1 with huIFNGR1 structures. The 2 structures of free and unbounded form of chIFNGR1 solved in this study colored in green, and the huIFNGR1 colored in yellow. Their overall structure is quite similar (shown on the *left* side). After rotation with an angle of 90°, with their first Ig domains superimposed, the second Ig domains are related by a 30.9° rotation. The colored dash lines represent the second Ig domains within the huIFNGR1 and chIFNGR1, respectively (seen in the *right* side).

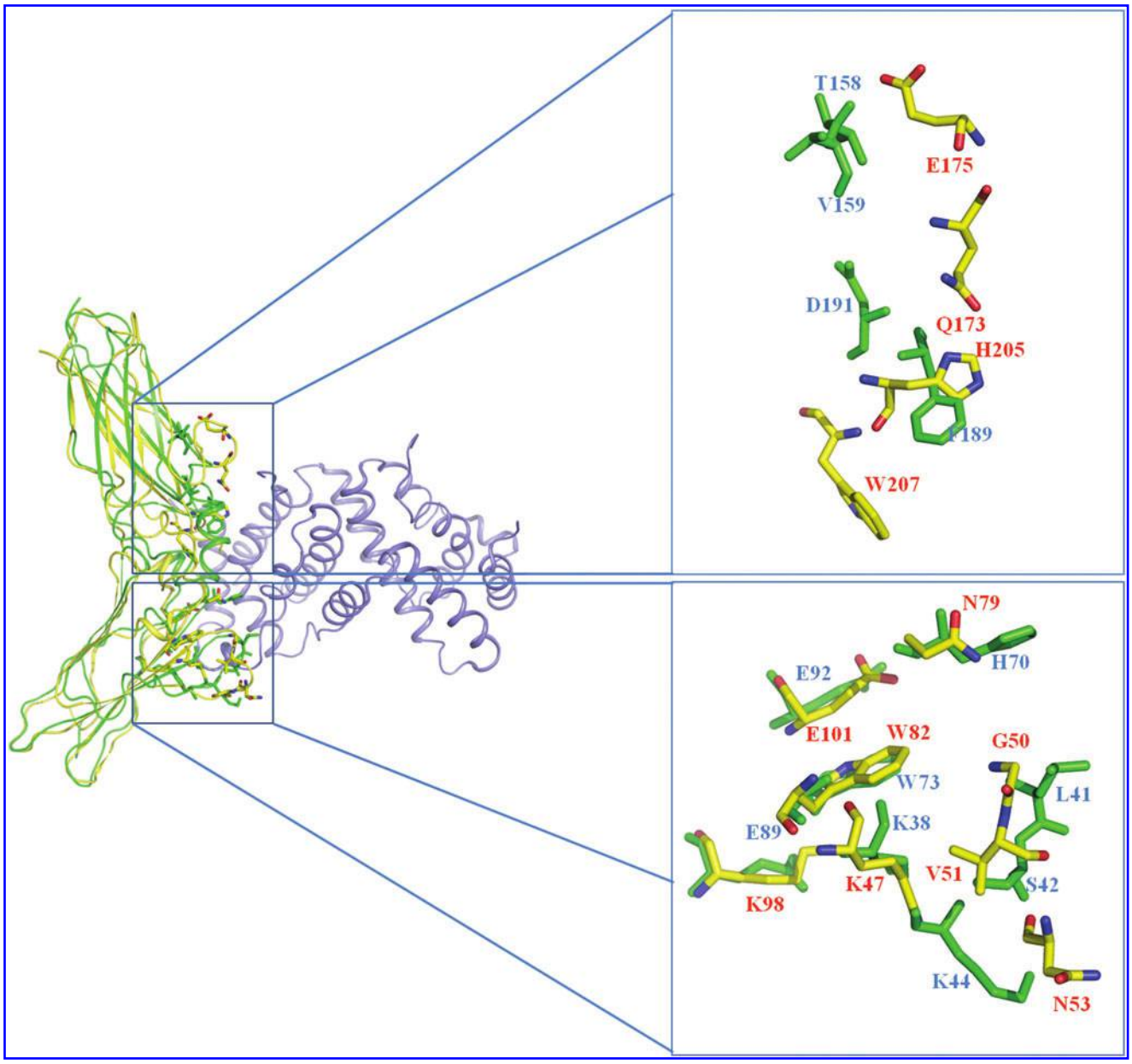

FIG. 6. Close-up view of the ligand–receptor binding sites comparison between chIFNGR1 and huIFNGR1. The binding sites of huIFN-γ &huIFNGR1 complex were analyzed and marked with yellow sticks, and the green ones represent the counterpart sites in chIFNGR1. chIFNGR1 (green), huIFNGR1 (yellow), huIFN-γ (blue).

We also applied SPR using Biacore 3000 to detect the binding affinity of chIFN-γ with chIFNGR1. SPR is an optical technique that has gained wide recognition as a valuable tool to investigate biological interactions. SPR offers real-time *in situ* analysis of dynamic surface events and thus, is capable of defining the rates of both adsorption and desorption for a range of surface interactions (Green and others 2000). First, chIFNGR1 was immobilized onto CM5 sensor surface with ~1,500 RU. Then gradient concentration (0, 31.25, 62.5, 125, and 250 nM) of chIFN-γ was injected, and the data were real-time recorded (Fig. 8). ChIFN-γ exhibited dramatically high binding affinity ($K_D = 2.3 \times 10^{-8}$ M) to chIFNGR1, and the kinetic data (k_{on} was 1.25×10^5 $M^{-1} \cdot s^{-1}$ and k_{off} was 2.68×10^{-3} s^{-1}) fit well with the 1:1 binding model, which was consistent with the size-exclusion chromatography assay. The putative binding sites of chIFNGR1 to chIFN-γ were prepared using site-directed mutagenesis method, and purified like the wild-type chIFNGR1 (Fig. 9a). The analysis result of the binding property of those mutations to chIFN-γ using SPR indicated that the K38A, L41A, H70A, E92A, F189A, and D191A mutations had no binding capability to chIFN-γ; however, the other mutations S42A, K44A, W73A, E89A, T158A, and V159A still could bind to chIFN-γ (Fig. 9b), the binding parameters was shown in Table 3.

Discussion

The activation of numerous cytokines relies on ligand–receptor association, which is responsible for the initiation of signaling transduction pathway cascades (Platanias 2005;

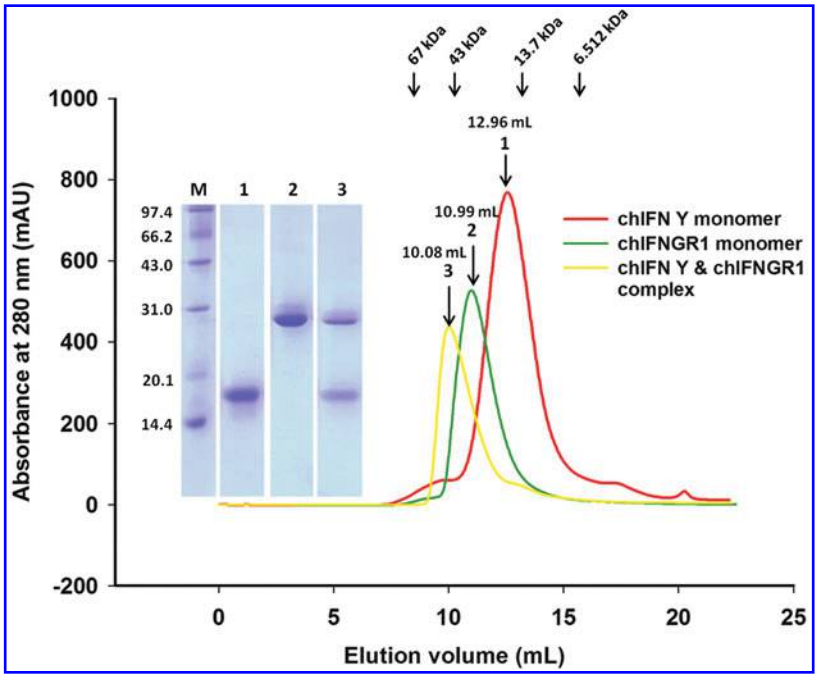

FIG. 7. The elution profiles of chIFN-γ, chIFNGR1, chIFN-γ and chIFNGR1 complex were displayed by size-exclusion chromatograph, which was carried out with a Superdex™ 75 10/300 GL column (GE Healthcare). The molecular weight of elution volume was marked according to the instructions of the column, and elution volume of every peak was labeled on the top of them. 15% sodium dodecyl sulfate polyacrylamide gel electrophoresis (SDS-PAGE) results showed that the correct molecular weight of chIFN-γ and chIFNGR1 monomers, and they could bind with each other with 1:1 ratio. The molecular weight of chIFN-γ and chIFNGR1 are 17 and 24 kDa, respectively, which are correspondent with their elution volume of size-exclusion chromatography.

Sadler and Williams 2008). Here we expressed the recombinant chIFN-γ and one of its receptor chIFNGR1 in prokaryotic cell (*E. coli*) as soluble proteins and inclusion bodies, respectively.

In contrast to the dimerization IFN-γ of other species (Ealick and others 1991; Samudzi and others 1991; Randal and Kossiakoff 2000), chicken IFN-γ form monomers according to the elusion volume of size-exclusion chromatography (Fig. 7), and binds to chIFNGR1 with 1:1 ratio, which was confirmed by the Biacore 3000 SPR and possessed high binding affinity ($K_D = 2.3 \times 10^{-8}$ M), approaching to the ligand–receptor binding affinity ($K_D = 10^{-9}$–10^{-10} M) of huIFN-γ to huIFNGR1 (Marsters and others 1995; Walter and others 1995). Moreover, further investigation using size-exclusion chromatography supported the result of SPR. All of this information suggests that chIFN-γ, like huIFN-γ, could bind to the alpha chain of its receptor (chIFNGR1) with high affinity with a 1:1 mode. However, the diversity of species results in the difference form of the configuration of their ligand: monomerization to chIFN-γ and the dimerization of huIFN-γ.

Interestingly, although there is only low sequence conservation between chIFNGR1 with other class II cytokine receptors, such as human IFNGR1 (huIFNGR1), human IL-10R1 (huIL-10R1), and human IL-22R1 (huIL-22R1) the structural comparison demonstrated that the chIFNGR1 shares tremendous similarity with other cytokine receptors. After superimposing the chIFNGR1 to huIFNGR1& huIFN-γ

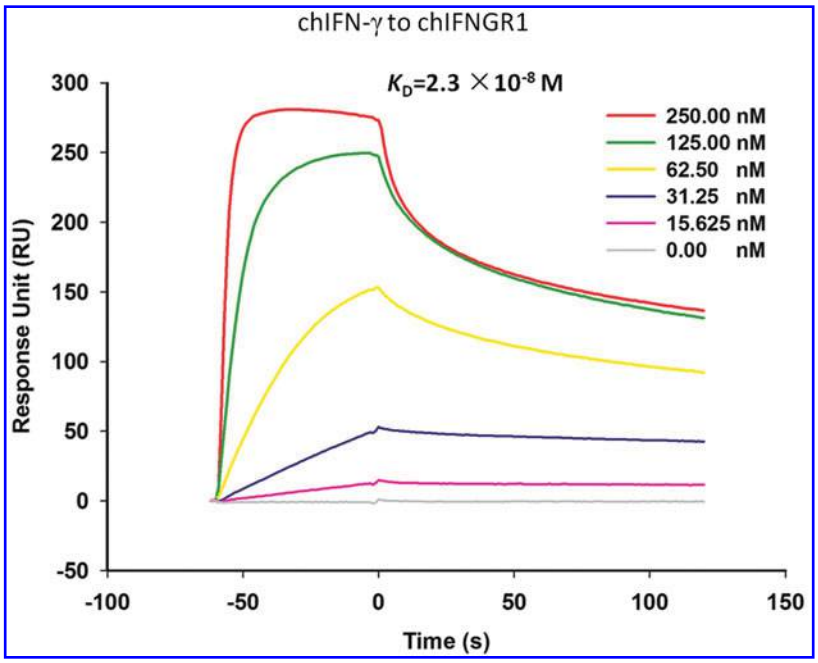

FIG. 8. Surface plasmon resonance measurement of chIFN-γ monomer binding to immobilized chIFNGR1 monomer. chIFNGR1 was immobilized on the CM5 sensor chip with ~1,500 RU. chIFN-γ protein was injected as mobile phase with the concentration of 15.625, 31.25, 62.50, 125.00, and 250.00 nM. All injections were performed at 25°C and measured using Biacore 3000 instrument (GE Healthcare). Kinetics analysis was carried out using the BIAevaluation software version 4.1, and then fit by assuming a simple 1:1 Langmuir binding model. The K_D of chIFNGR1 to chIFN-γ was 2.3×10^{-8} M.

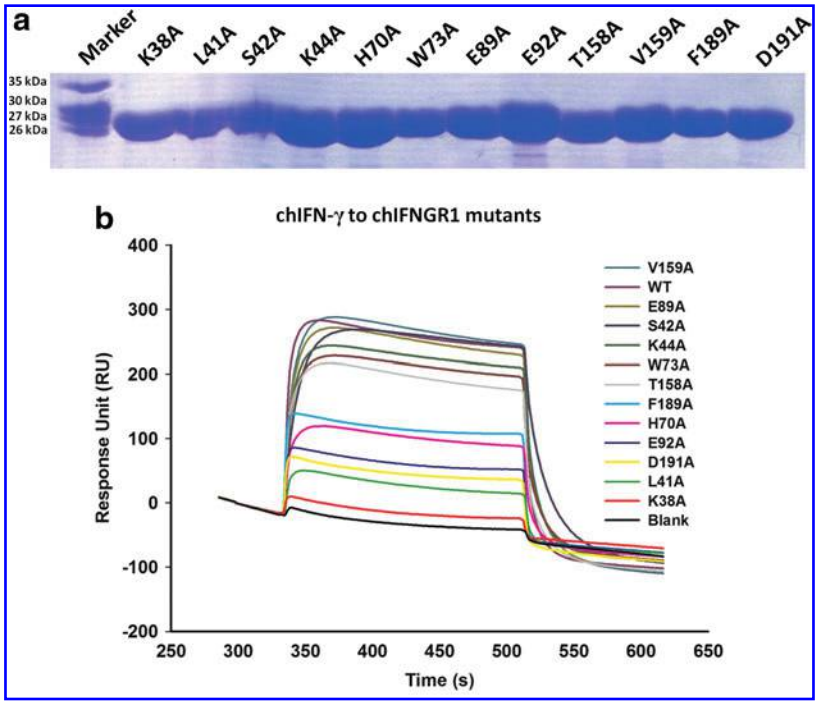

FIG. 9. The purification of chIFNGR1 mutations and their binding capacities to chIFN-γ. **(a)** SDS-PAGE of purified chIFNGR1 mutations. All of the mutations were purified by inclusion body refolding as the wild type and all of them were diluted to 1 μM for surface plasmon resonance analysis. **(b)** Binding property of chIFNGR1 mutations with chIFN-γ. With the immobilization of His_4 monoclonal antibody (mAb) into the CM5 sensor chip, chIFN-γ with N-terminal His-tag could bind to His antibody and the complexes were eluted by phosphoric acid, mutant chIFNGR1 was injected and the binding property of different chIFNG1 mutations was detected by the Biacore 3000 system one after another.

complex, the superimposed majority binding sites of the complex provided evidence for the chIFNGR1 binding sites in the structural level. It could be inferred that the binding sites of chIFNGR1 to its ligand could be focused on those sites, although there is no structure solved for the chIFNGR1& chIFN-γ complex.

In conclusion, the monomer of chIFN-γ and chIFNGR1 could bind each other with high affinity and a 1:1 binding mode. Moreover, the structural superimposition of chIFNGR1 with the single crystal structure of other class II cytokine receptors and human IFN-γ&IFNGR1 complex indicates the similar structure of chicken chIFNGR1 and other cytokine receptors. Further, chIFNGR1 shares the same binding sites with the huIFNGR1 to chIFN-γ, which provides structural evidence for chIFNGR1 binding to its ligand chIFN-γ in a similar manner.

Table 3. Binding Property of chIFN-γ with chIFNGR1 Mutants

Mutants of chIFNGR1	*Immobilization of chIFN-γ (RU)*	*Binding of chIFNGR1(RU)*	*Binding (Yes/No)*
K38A	1,608	−80.0	No
L41A	1,589	−51.0	No
S42A	1,613	167.8	Yes
K44A	1,631	109.8	Yes
H70A	1,647	−20.0	No
W73A	1,673	73.6	Yes
E89A	1,689	96.7	Yes
E92A	1,703	−95.8	No
T158A	1,735	15.0	Yes
V159A	1,739	83.9	Yes
F189A	1,736	−91.6	No
D191A	1,740	17.4	No
WT	1,734	150.3	Yes

Acknowledgments

We thank the beamline scientists at Shanghai Synchrotron Radiation Facility (SSRF-beamline 17U) for technical support during data collection and Dr. Zheng Fan for assistance with SPR experiment. This work was supported by National Natural Science Foundation of China (NSFC; grant no. 31072118) and National Natural Science Foundation of China (NSFC; grant no. 81021003). Coordinates and structure factors are deposited in the Protein Data Bank (PDB code 4EQ2 for native chIFNGR1 and 4EQ3 for Se-Met chIFNGR1).

Author Disclosure Statement

No competing financial interests exist.

References

Adams PD, Grosse-Kunstleve RW, Hung LW, Ioerger TR, McCoy AJ, Moriarty NW, Read RJ, Sacchettini JC, Sauter NK, Terwilliger TC. 2002. PHENIX: building new software for automated crystallographic structure determination. Acta Crystallogr D Biol Crystallogr 58(Pt 11):1948–1954.

Aguet M, Dembic Z, Merlin G. 1988. Molecular cloning and expression of the human interferon-gamma receptor. Cell 55:273–280.

Bach EA, Szabo SJ, Dighe AS, Ashkenazi A, Aguet M, Murphy KM, Schreiber RD. 1995. Ligand-induced autoregulation of IFN-gamma receptor beta chain expression in T helper cell subsets. Science 270:1215–1218.

Begley MJ, Taylor GS, Kim SA, Veine DM, Dixon JE, Stuckey JA. 2003. Crystal structure of a phosphoinositide phosphatase, MTMR2: insights into myotubular myopathy and Charcot-Marie-Tooth syndrome. Mol Cells 12:1391–1402.

Bleicher L, de Moura PR, Watanabe L, Colau D, Dumoutier L, Renauld JC, Polikarpov I. 2008. Crystal structure of the IL-22/IL-22R1 complex and its implications for the IL-22 signaling mechanism. FEBS Lett 582:2985–2992.

Buchmeier NA, Schreiber RD. 1985. Requirement of endogenous interferon-gamma production for resolution of *Listeria monocytogenes* infection. Proc Natl Acad Sci U S A 82:7404–7408.

Chen Y, Liu P, Gao F, Cheng H, Qi J, Gao GF. 2010. A dimeric structure of PD-L1: functional units or evolutionary relics? Protein Cell 1:153–160.

Chene C, Fountoulakis M, Dobeli H, D'Arcy B, Winkler F, D'Arcy A. 1995. Crystallization of the complex of human IFN-gamma and the extracellular domain of the IFN-gamma receptor. Proteins 23:591–594.

Collaborative Computing Project Number 4. 1994. The CCP4 suite: programs for protein crystallography. Acta Crystallogr D Biol Crystallogr 50(Pt 5):760–763.

Cooper MA. 2003. Label-free screening of bio-molecular interactions. Anal Bioanal Chem 377:834–842.

DeLano WL. 2002. The PyMOL User's Manual. San Carlos, CA: Delano Scientific.

Digby MR, Lowenthal JW. 1995. Cloning and expression of the chicken interferon-gamma gene. J Interferon Cytokine Res 15:939–945.

Ealick SE, Cook WJ, Vijay-Kumar S, Carson M, Nagabhushan TL, Trotta PP, Bugg CE. 1991. Three-dimensional structure of recombinant human interferon-gamma. Science 252:698–702.

Emsley P, Cowtan K. 2004. Coot: model-building tools for molecular graphics. Acta Crystallogr D Biol Crystallogr 60(Pt 12 Pt 1):2126–2132.

Farrar MA, Schreiber RD. 1993. The molecular cell biology of interferon-gamma and its receptor. Annu Rev Immunol 11: 571–611.

Fountoulakis M, Zulauf M, Lustig A, Garotta G. 1992. Stoichiometry of interaction between interferon gamma and its receptor. Eur J Biochem 208:781–787.

Gao Q, Nie P, Thompson KD, Adams A, Wang T, Secombes CJ, Zou J. 2009. The search for the IFN-gamma receptor in fish: functional and expression analysis of putative binding and signalling chains in rainbow trout *Oncorhynchus mykiss*. Dev Comp Immunol 33:920–931.

Grayfer L, Belosevic M. 2009. Molecular characterization of novel interferon gamma receptor 1 isoforms in zebrafish (*Danio rerio*) and goldfish (*Carassius auratus* L.). Mol Immunol 46:3050–3059.

Green RJ, Frazier RA, Shakesheff KM, Davies MC, Roberts CJ, Tendler SJB. 2000. Surface plasmon resonance analysis of dynamic biological interactions with biomaterials. Biomaterials 21:1823–1835.

Han CL, Zhang W, Dong HT, Han X, Wang M. 2006. A novel gene of beta chain of the IFN-gamma receptor of Huiyang chicken: cloning, distribution, and CD assay. J Interferon Cytokine Res 26:441–448.

Han X, Chen T, Wang M. 2008. Molecular cloning and characterization of chicken interferon-gamma receptor alpha-chain. J Interferon Cytokine Res 28:445–454.

Hendrickson WA, Horton JR, LeMaster DM. 1990. Selenomethionyl proteins produced for analysis by multiwavelength anomalous diffraction (MAD): a vehicle for direct determination of three-dimensional structure. EMBO J 9: 1665–1672.

Josephson K, Logsdon NJ, Walter MR. 2001. Crystal structure of the IL-10/IL-10R1 complex reveals a shared receptor binding site. Immunity 15:35–46.

Kotenko SV. 2002. The family of IL-10-related cytokines and their receptors: related, but to what extent? Cytokine Growth Factor Rev 13:223–240.

Lake BD, Steward CG, Oakhill A, Wilson J, Perham TG. 1997. Bone marrow transplantation in late infantile Batten disease and juvenile Batten disease. Neuropediatrics 28:80–81.

Langer JA, Cutrone EC, Kotenko S. 2004. The Class II cytokine receptor (CRF2) family: overview and patterns of receptor-ligand interactions. Cytokine Growth Factor Rev 15:33–48.

Laskowski RA, Macarthur MW, Moss DS, Thornton JM. 1993. Procheck—a program to check the stereochemical quality of protein structures. J Appl Cryst 26:283–291.

Marsters SA, Pennica D, Bach E, Schreiber RD, Ashkenazi A. 1995. Interferon gamma signals via a high-affinity multisubunit receptor complex that contains two types of polypeptide chain. Proc Natl Acad Sci U S A 92:5401–5405.

Miknis ZJ, Magracheva E, Li W, Zdanov A, Kotenko SV, Wlodawer A. 2010. Crystal structure of human interferon-lambda1 in complex with its high-affinity receptor interferon-lambdaR1. J Mol Biol 404:650–664.

Mosmann TR, Coffman RL. 1989. TH1 and TH2 cells: different patterns of lymphokine secretion lead to different functional properties. Annu Rev Immunol 7:145–173.

Murshudov GN, Vagin AA, Dodson EJ. 1997. Refinement of macromolecular structures by the maximum-likelihood method. Acta Crystallogr D Biol Crystallogr 53(Pt 3):240–255.

Perussia B. 1991. Lymphokine-activated killer cells, natural killer cells and cytokines. Curr Opin Immunol 3:49–55.

Ping Z, Shi Y, Sun Y, Ma L, Wang M. 2012. Protein expression, crystallization and preliminary X-ray crystallographic analysis of chicken interferon-gamma receptor alpha chain. Acta Crystallogr Sect F Struct Biol Cryst Commun 68(Pt 1): 41–44.

Platanias LC. 2005. Mechanisms of type-I- and type-II-interferon-mediated signalling. Nat Rev Immunol 5:375–386.

Portnoy DA. 1992. Innate immunity to a facultative intracellular bacterial pathogen. Curr Opin Immunol 4:20–24.

Randal M, Kossiakoff AA. 2000. The 2.0 A structure of bovine interferon-gamma; assessment of the structural differences between species. Acta Crystallogr D Biol Crystallogr 56(Pt 1): 14–24.

Read RJ. 2001. Pushing the boundaries of molecular replacement with maximum likelihood. Acta Crystallogr D Biol Crystallogr 57(Pt 10):1373–1382.

Rich RL, Hoth LR, Geoghegan KF, Brown TA, LeMotte PK, Simons SP, Hensley P, Myszka DG. 2002. Kinetic analysis of estrogen receptor/ligand interactions. Proc Natl Acad Sci U S A 99:8562–8567.

Sad S, Marcotte R, Mosmann TR. 1995. Cytokine-induced differentiation of precursor mouse CD8+ T cells into cytotoxic CD8+ T cells secreting Th1 or Th2 cytokines. Immunity 2: 271–279.

Sadler AJ, Williams BR. 2008. Interferon-inducible antiviral effectors. Nat Rev Immunol 8:559–568.

Samudzi CT, Burton LE, Rubin JR. 1991. Crystal structure of recombinant rabbit interferon-gamma at 2.7-A resolution. J Biol Chem 266:21791–21797.

Savan R, Ravichandran S, Collins JR, Sakai M, Young HA. 2009. Structural conservation of interferon gamma among vertebrates. Cytokine Growth Factor Rev 20:115–124.

Sitlani A, Fisher TS, Lo Surdo P, Pandit S, Mattu M, Santoro JC, Wisniewski D, Cummings RT, Calzetta A, Cubbon RM, Fischer PA, Tarachandani A, De Francesco R, Wright SD, Sparrow CP, Carfi A. 2007. Effects of pH and low density lipoprotein (LDL) on PCSK9-dependent LDL receptor regulation. J Biol Chem 282:20502–20512.

Song KD, Lillehoj HS, Choi KD, Zarlenga D, Han JY. 1997. Expression and functional characterization of recombinant chicken interferon-gamma. Vet Immunol Immunopathol 58: 321–333.

Suzuki Y, Orellana MA, Schreiber RD, Remington JS. 1988. Interferon-gamma: the major mediator of resistance against *Toxoplasma gondii*. Science 240:516–518.

Thiel DJ, le Du MH, Walter RL, D'Arcy A, Chene C, Fountoulakis M, Garotta G, Winkler FK, Ealick SE. 2000. Observation of an unexpected third receptor molecule in the crystal structure of human interferon-gamma receptor complex. Structure 8:927–936.

Walter MR, Windsor W, Nagabhushan TL, Lundell DJ, Lunn CA, Zauodny PJ, Narula SK. 1995. Crystal structure of a complex between interferon-gamma and its soluble high affinity receptor. Nature 376:230–235.

Wei D, Li M, Zhang X, Xing L. 2004. An improvement of the site-directed mutagenesis method by combination of megaprimer, one-side PCR and DpnI treatment. Anal Biochem 331:401–403.

Address correspondence to:
Dr. Ming Wang
College of Veterinary Medicine
China Agricultural University
No. 2 Yuan Ming Yuan West Road
Hai-dian District
Beijing, 100193
China

E-mail: vetdean@cau.edu.cn

or

Dr. George F. Gao
Institute of Microbiology, Chinese Academy of Sciences
No.1 Beichen West Road
Chao-yang District
Beijing 100101
China

E-mail: gaof@im.ac.cn

Received 11 December 2012/Accepted 10 June 2013